2019

Role of Bismuth in the Stability of Pt-Bi Bimetallic Catalyst for Methane Mediated Deoxygenation of Guaiacol, an APXPS study

Yang Xiao, *Louisiana Tech University*

ACS Catalysis

Research Article

Cite This: ACS Catal. 2019, 9, 3694−3699

pubs.acs.org/acscatalysis

Role of Bismuth in the Stability of Pt−Bi Bimetallic Catalyst for Methane Mediated Deoxygenation of Guaiacol, an APXPS Study

Kanak Roy,[†] Luca Artiglia,[*,‡,§] Yang Xiao,[∥] Arvind Varma,[∥] and Jeroen A. van Bokhoven[†,‡]

[†]Institute for Chemical and Bioengineering, ETH Zürich, 8093 Zurich, Switzerland

[‡]Laboratory for Catalysis and Sustainable Chemistry, Paul Scherrer Institute, Forschungsstrasse 111, 5232 Villigen, Switzerland

[§]Laboratory of Environmental Chemistry, Paul Scherrer Institute, Forschungsstrasse 111, 5232 Villigen, Switzerland

[∥]Davidson School of Chemical Engineering, Purdue University, West Lafayette, Indiana 47907, United States

Supporting Information

ABSTRACT: Catalytic deoxygenation, that is, the removal of oxygen over heterogeneous catalysts, is used as a strategy of upgrading bio-oils into fuels. Until now, the most commonly studied and used reagent has been hydrogen. Substituting hydrogen with methane is a cost-effective and smart strategy, because methane is abundant as the principal component of natural gas and shale gas. In this paper we used methane as a direct source of hydrogen for the deoxygenation of guaiacol over activated carbon supported platinum−bismuth bimetallic catalysts. The promotional effect of bismuth was investigated using in situ ambient-pressure X-ray photoelectron spectroscopy on these particulate catalysts. In comparison to the catalyst containing only platinum, bismuth hinders platinum oxidation, stabilizing it in the metallic state both before and after prereduction in hydrogen. Guaiacol strongly interacts with bismuth, which partially oxidizes in the presence of the mild oxygenate, and carbonyl species accumulate on the surface. In the absence of bismuth, coke formation and sintering prevail.

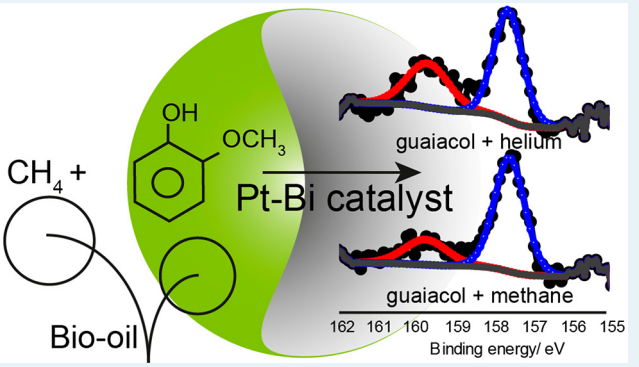

KEYWORDS: *ambient-pressure X-ray photoelectron spectroscopy, bio-oil, guaiacol, methane, platinum−bismuth, deoxygenation*

INTRODUCTION

A significant replacement of petroleum fuels with biofuels, i.e. fuels derived from biomass, is a major move toward sustainability. Pyrolysis of lignocellulosic biomass has been devised as a good strategy to obtain liquid bio-oils.[1] However, direct utilization of bio-oil into transportation fuels has been challenging owing to its high oxygen content, which is about 50%, much higher than that in crude oil.[2] This leads to unwanted properties, including low heating value, high viscosity, and immiscibility with hydrocarbon fuels. Catalytic hydrodeoxygenation (HDO), which refers to the removal of oxygen by hydrogen over heterogeneous catalysts, is used as a strategy of upgrading bio-oils into fuels.[1−9] Substituting hydrogen with methane[10] is a cost-effective alternative and smart strategy, since methane is abundant as the principal component of natural gas and shale gas. In addition, largely owing to transportation costs, tons of methane are flared at the oil-extraction sites annually. As hydrogen is typically manufactured from methane by steam reforming, a direct use of methane as a source of hydrogen has decisive advantage.

Due to the complex nature and composition of pyrolysis bio-oils, guaiacol (2-methoxyphenol) is typically selected as a representative model compound for HDO studies. Guaiacol contains two common oxygenated groups, aromatic bonded methoxy and phenolic oxygen.[11] On one of the key catalysts, 5% Pt supported on activated carbon (Pt/AC), methane shows deoxygenation performance comparable to that of hydrogen in terms of guaiacol conversion and product distribution. The effectiveness of methane as a reductant drives the need for improvement of the catalyst, as the catalyst undergoes severe deactivation within 3 h of time on stream (TOS) in methane. With the addition of bismuth, the lifetime of the Pt-Bi/AC catalyst is extended without any significant drop in the activity or change in product distribution. Previous reaction and kinetic studies explored the optimum operating conditions and reaction pathways for guaiacol deoxygenation using methane.[10,12,13] The positive effect of bismuth is clear; however, the origin of this is not.

Bismuth is known for displaying promoting effects in association with noble metals such as palladium and platinum for the selective liquid-phase oxidation of alcohols, aldehydes, and carbohydrates with molecular oxygen.[14−19] Many interpretations of bismuth promotion, mainly based on liquid-phase selective oxidation, are available, which include geometric

Received: November 22, 2018
Revised: February 12, 2019
Published: March 18, 2019

DOI: 10.1021/acscatal.8b04699
ACS Catal. 2019, 9, 3694−3699

blocking of a fraction of active sites on the noble metal, stabilization of metallic platinum, that is, during the reaction bismuth would be in a higher oxidation state and protect platinum or palladium from oxidation, decrease in metal corrosion in the acidic solution, and formation of surface complexes among an α-functionalized alcohol, a positively charged bismuth atom or ion, and a surface palladium or platinum atom. However, studies on bismuth promotion in bio-oil deoxygenation are scarce. The vast majority of studies use model systems, which provide insights into actual catalysts depending on the quality of the model. Here, we show that ambient-pressure X-ray photoelectron spectroscopy (APXPS), which is a well-established method applied in the analysis of actual catalysts and in electrochemistry,[20−23] can be used to investigate the reactivity toward complex reactants having practical applications, such as guaiacol.

Herein, we determine the role of bismuth in improving the stability of Pt/AC catalysts.[10] By means of APXPS,[21,22,24,25] we investigate the reaction of guaiacol and methane over two active catalysts, i.e. 5 wt % Pt/AC and 5 wt % Pt-2 wt % Bi/AC. Since only these two catalysts were used in the present work, in later sections weight basis and AC support are not noted explicitly when describing them. Thus, the Pt and PtBi catalysts refer to 5 wt % Pt/AC and 5 wt % Pt-2 wt % Bi/AC, respectively. The results show that bismuth is oxidized to a high extent during the exposure to guaiacol and acts as a cocatalyst of the Pt-Bi bimetallic sites. These findings suggest the importance of bismuth in promoting the overall performance of the catalyst.

RESULTS AND DISCUSSION

The characterization information on the catalysts, including surface area, particle size, Pt dispersion, and bismuth loading, is available in Tables S1−S3 in the Supporting Information. The same catalysts have already been described in ref 10, and transmission electron microscopy (TEM) images of fresh and used samples described in this work, showing comparable metal particle size and dispersion, are shown in Figure S1. It appears that on PtBi nanoparticles the morphology essentially remains the same after reaction tests in comparison with fresh samples. The performance of Pt and PtBi (guaiacol conversion as a function of the time on stream) is shown in Figure S2. The results are in agreement with ref 10. On the Pt catalyst the guaiacol conversion starts to decrease immediately. After the first 2 h on stream it decreases from 80% to 70% and reaches ca. 20% after 6 h. Conversely on PtBi the conversion of guaiacol is stable at around 60% over the investigated time on stream (12 h). The guaiacol conversion measured on a 2% Bi/AC catalyst, used as a reference, demonstrates that platinum is necessary to catalyze the deoxygenation reaction.

In the APXPS experiment, a mixture of gaseous methane and guaiacol vapors (molar ratio 9:1, based on the partial pressure of the gases detected in the experimental cell) was dosed into the reaction cell. The pressure during the experiment was kept constant at 1 mbar, at a constant temperature of 673 K. XPS measurements were performed using linearly polarized light at a photon energy of 650 eV. The photon source was the X07DB In Situ Spectroscopy bending magnet soft X-ray (250−1800 eV) beamline, at the Swiss Light Source synchrotron.[26] Figure 1 shows the Bi $4f_{7/2}$ core level spectra of the PtBi catalyst recorded at 673 K at a total pressure of 1 mbar under steady state and various conditions. At first, the spectra were recorded in a helium environment, after which the catalyst was activated

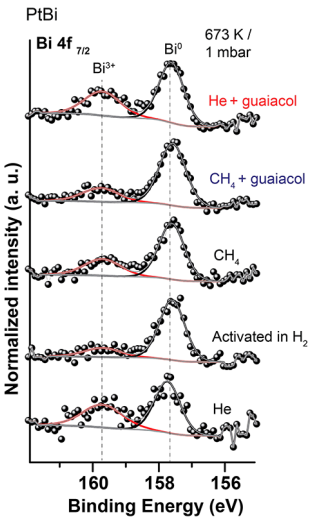

Figure 1. Bi $4f_{7/2}$ signals of PtBi catalyst recorded at 673 K and at a total pressure of 1 mbar at various conditions. Spectra were acquired with the excitation photon energy $h\nu$ = 650 eV.

in hydrogen for 4 h. The Bi $4f_{7/2}$ signal shows two peaks at 157.6 and at 159.7 eV, which correspond to metallic (Bi^0) and cationic bismuth (Bi^{3+}) species, respectively. The ratio of Bi^{3+} and Bi^0 in the hydrogen activated catalyst is 0.21. In methane, and in the mixture of methane and guaiacol, the oxidic component increases slightly and the ratio is 0.25. Next, the methane was switched off, while the guaiacol flow was kept constant. The total pressure was balanced to 1 mbar using helium. The Bi^{3+} component (159.7 eV) increases significantly and the Bi^{3+}/Bi^0 ratio reaches a value of 0.58. The results suggest that bismuth acts as a high affinity site for guaiacol, in comparison to platinum. The high vulnerability of bismuth to oxidation is in fact well reported[27] in the presence of oxygen for selective oxidation of alcohols. There, it acts as a cocatalyst due to its high affinity toward oxygen, protecting platinum active metal from oxidation.[28] However, no report on in situ oxidation of bismuth in the presence of only a mild oxygenate (such as guaiacol) has been shown previously. Figure S3 shows that the Pt 4f signals acquired under various conditions do not display any abrupt change after the activation of both the Pt and PtBi catalysts in hydrogen. In the case of PtBi, the amount of cationic platinum is relevant before activation (Pt^{2+}/Pt^0 = 0.45, see the table in Figure S3) and decreases considerably after activation in hydrogen (0.26). In the case of the Pt sample, the line shape of the Pt 4f signal does not show any relevant variation. After pretreatment in hydrogen, the Pt^{2+}/Pt^0 ratio stabilizes at around 0.45 and 0.20 for Pt and PtBi, respectively.

It is to be underscored that the amount of metallic platinum (Pt^0) in PtBi is higher in comparison to that of Pt, supporting the hypothesis that bismuth protects the metallic platinum from oxidation (see table in Figure S3). Figure 2 shows the time evolution of the Bi^{3+}/Bi^0 ratio of the PtBi catalyst in a 40 min timespan. Table 1 shows the Bi^{3+}/Bi^0 ratio evaluated from XPS under different reaction conditions and during a 30 min exposure to a mixture of helium and guaiacol. While the flow between CH_4 + guaiacol and He + guaiacol was quickly replaced, spectra were recorded in cycles where a single spectrum of the Bi 4f was acquired in 17 s. In the ambient-pressure cell of our APXPS setup, a complete exchange of gases is possible in less than 10 s.[25] Each point in the plot

DOI: 10.1021/acscatal.8b04699
ACS Catal. 2019, 9, 3694−3699

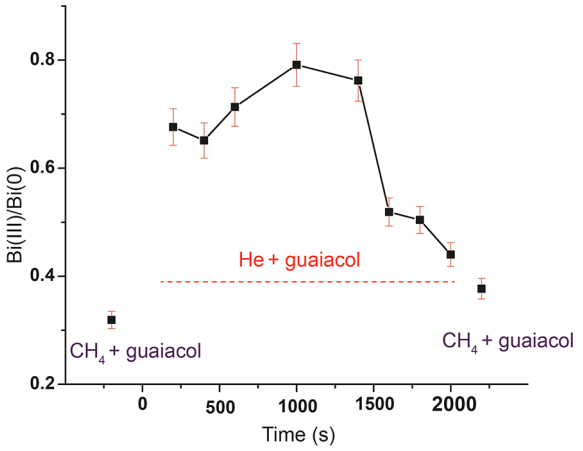

Figure 2. Evolution with time of the Bi^{3+}/Bi^0 in the PtBi catalysts recorded at 673 K and at a total pressure of 1 mbar after switching from CH_4 + guaiacol to a mixture of He + guaiacol. Spectra were acquired with the excitation photon energy $h\nu$ = 650 eV.

Table 1. Evolution of the Bi^{3+}/Bi^0 Ratio in Different Reaction Conditions and as a Function of Time during Exposure to Helium + Guaiacol (Figure 2)

conditions	Bi^{3+}/Bi^0
unactivated catalyst in helium	0.64
catalyst activated in H_2	0.21
CH_4	0.26
CH_4 + guaiacol	0.31
helium + guaiacol	
200 s	0.68
400 s	0.65
600 s	0.61
1000 s	0.79
1400 s	0.76
1600 s	0.52
1800 s	0.50
2000 s	0.44

corresponds to a sum of 8 spectra of Bi 4f, corresponding to 136 s. In CH_4 + guaiacol, the Bi^{3+}/Bi^0 ratio in the catalyst is 0.25. After methane is replaced by helium, the Bi^{3+}/Bi^0 ratio increases to 0.75 within 1000 s. The amount of cationic bismuth then decreases and stabilizes at around 0.45 after 2000 s of the exposure. Oscillations of the Bi^{3+}/Bi^0 ratio between 0.4 and 0.5 observed after 1500 s are likely a result of the Bi $4f_{7/2}$ deconvolution procedure. In order to explain such an effect, we evaluated the evolution of the Pt 4f/C 1s (hereafter called Pt/C), Bi 4f/C 1s (hereafter called Bi/C), and Pt 4f/Bi 4f (hereafter called Pt/Bi) ratios in the PtBi sample and the evolution of the Pt/C ratio in the Pt sample as a function of the reaction conditions. The results are shown in Figure S4. The Pt/Bi ratio of the "as introduced" sample (measured at room temperature and 1.0 mbar helium background pressure) is 0.86, proving that the surface composition of the nanoparticles is almost 1:1 (Pt:Bi). Energy dispersive X-ray analysis of transmission electron microscopy images (EDX-TEM) in Figure S5 show that the distribution of Pt and Bi in the nanoparticles is homogeneous both in the "as introduced" PtBi sample and after reaction with a CH_4 + guaiacol mixture. The phase equilibrium diagram of the platinum−bismuth system shows that a $PtBi_2$ composition would be expected at room temperature.[29] The Pt/Bi ratio increases considerably upon increasing the temperature to 400 °C in helium. In addition, the Pt/C and Bi/C ratios are increased, the latter considerably less than the former. This suggests that an increase in the temperature in helium background

(i) "cleans" the nanoparticles, most likely favoring desorption of residual chemisorbed gas molecules (e.g., water, carbon monoxide), partially attenuating the photoemission signals

(ii) promotes the surface segregation of platinum

The Pt/Bi ratio keeps decreasing almost constantly until a reductant is present and again reaches the starting value (0.86) in the reaction mixture (CH_4 + guaiacol). When methane is removed from the reaction mixture, the ratio decreases significantly, from 0.86 to 0.58.

The Pt/C and Bi/C ratios behave similarly. Upon dosing of hydrogen their values decrease to the initial (room temperature, 1.0 mbar He) levels, while they are stable in the gas mixtures containing a reductant. The Pt/C ratio starts to decrease again in the presence of He + guaiacol. Taken together, the results of Figure S4a indicate that bimetallic Pt-Bi nanoparticles are stable after the activation at 400 °C in hydrogen. The behavior of the Pt/C and Bi/C ratios shows that neither a metal diffusion in the carbon support nor relevant coke formation takes place on PtBi, in good agreement with Table S4 and with Figures S1 and S6. The surface composition of the nanoparticles is mainly influenced by the temperature, and after an initial surface segregation of platinum at 400 °C in helium, the starting Pt:Bi atomic percentage is gradually recovered in the presence of a reductant (in the CH_4 + guaiacol reaction mixture the Pt/Bi ratio is 0.86) . Once methane is removed from the reaction mixture, bismuth surface enrichment is observed. We want to stress that the measurements shown in Figure S4a were carried out under steady-state conditions: i.e., the photoemission signals were not changing with time. The time-resolved evolution of Bi $4f_{7/2}$ within the first 30 min (Figure 2) on switching from CH_4 + guaiacol to He + guaiacol can be explained by a change in the surface atomic composition of the nanoparticles in the absence of a reductant. Approximately 25 min may be the time required for Bi to segregate and react with guaiacol to form a stable oxide layer.

As shown in Figure S6 and Table S4 of the Supporting Information, carbon deposition and coke formation are believed to be responsible for deactivation of the catalysts in guaiacol deoxygenation using methane as reductant. Indeed, temperature-programmed oxidation (TPO) performed on the used Pt and PtBi catalysts shows carbon dioxide production in both systems (Figure S4) between 300 and 600 °C. Similar results have been reported in the literature for reactions involving methane as a reactant.[30−32] For this reason, we show the C 1s photoemission signal acquired under different reaction conditions. Figure 3 displays a comparison of the C 1s signals acquired in situ on the Pt and PtBi catalysts. The spectra were deconvoluted with three components, located at 285.0, 286.3, and 287.5 eV, respectively. An additional component at 286.6 eV, corresponding to gas-phase methane, was added when methane was present in the mixture. The functional states correspond to sp^3 carbon (C−C, C−H) at 285 eV, hydroxyls or ethers (C−O and C−O−C) at 286.3 eV, and carbonyls (C═O) at 287.5 eV.[33] The peaks were quantified by calculating the integrated peak area. The amount of coke cannot be quantified independently, as the reported

DOI: 10.1021/acscatal.8b04699
ACS Catal. 2019, 9, 3694−3699

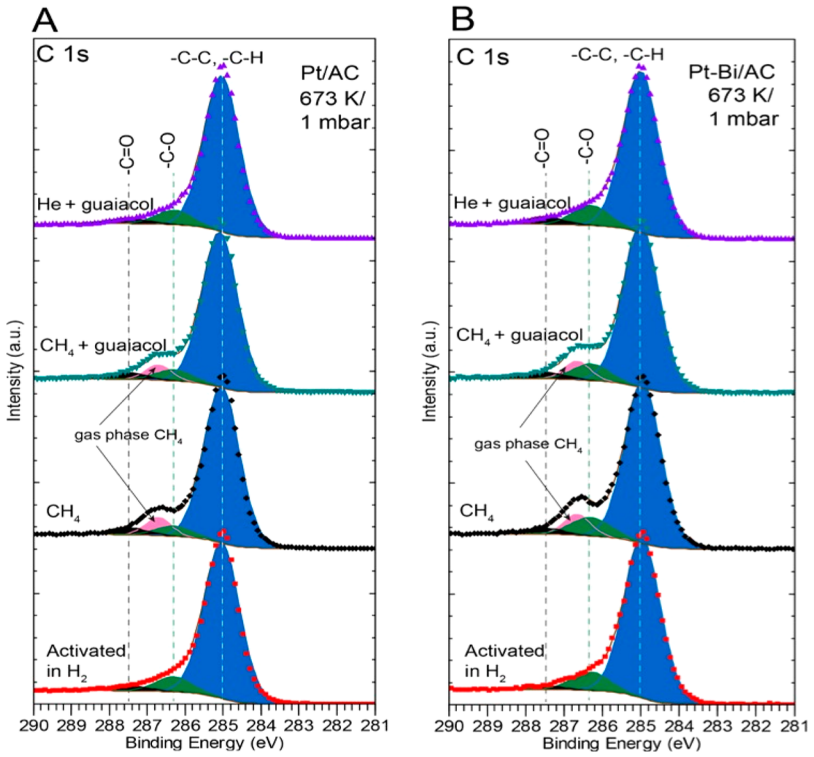

Figure 3. C 1s signals of (A) Pt/AC and (B) Pt-Bi/AC catalysts recorded at 673 K and at a total pressure of 1 mbar under various conditions. Spectra were acquired with the excitation photon energy $h\nu$ = 650 eV.

binding energy overlaps with that of the main peak of the AC substrate (sp^3 carbon) at 285.0 eV.[34,35] Therefore, we calculated the ratio between the area of the Pt 4f signal and that of the 285.0 eV component of the C 1s. If during the deoxygenation reaction carbon (coke) would accumulate on the surface, thus partially attenuating the photoemission signal coming from the metal, we would expect a decrease in the ratio. Figure S4b shows that the Pt/C ratio evaluated on the Pt sample decreases substantially when the temperature increases from room temperature to 400 °C in helium and then stabilizes during activation in hydrogen and in the presence of methane. It decreases again once methane is removed from the mixture. Therefore, on the Pt sample, both a temperature increase from room temperature to 400 °C in helium and the oxidizing reaction environment promote a decrease of the Pt/C ratio. Such an effect may be due to coke formation, to metal diffusion in the carbon support, or to the sintering of the nanoparticles. On the basis of the TPO data (Table S4 and Figure S6), showing coke accumulation on the Pt used sample, and on TEM and H_2−O_2 titration results (Figure S1 and Table S3), displaying a small increase in the Pt nanoparticle size upon reaction (from 4.2 to 4.9 nm), coke formation and sintering of the nanoparticles may prevail and influence the observed behavior of the Pt/C.

Overall, bimetallic platinum−bismuth nanoparticles are more stable than pure platinum nanoparticles. The TEM-EDX results in Figure S5 demonstrate that both Pt and Bi metals were observed in nanoparticles for fresh and used catalysts, indicating the formation of a bimetallic alloy. In fact, an alloy having a surface atomic ratio close to 1:1 forms both in the presence of a reductant and in the reaction mixture (CH_4 + guaiacol), and the amount of cationic platinum does not increase. In the presence of the oxidant (He + guaiacol), bismuth segregates at the surface of the nanoparticles, hindering the oxidation of platinum and limiting the formation of coke. The above observations prove that coke formation contributes to the deactivation of the Pt catalyst, while the addition of bismuth prevents such an effect. The amount of carbonyl species (287.5 eV, black peak in Figure 3) detected on PtBi is higher than on Pt. The C═O peak in the PtBi catalyst grows when the reactants are switched from a mixture of CH_4 + guaiacol to He + guaiacol, whereas in the case of the Pt catalyst, the C═O component remains stable throughout the switching cycles. The presence of bismuth may protect the catalyst from the accumulation of coke, leading to formation of other byproducts containing the carbonyl function and preventing fast deactivation.

CONCLUSIONS

From the analysis of the core-level peaks and time-resolved experiments of the Bi 4f photoemission signal on a bimetallic PtBi catalyst during the methane-mediated deoxygenation of guaiacol, we have shown that under oxidizing conditions bismuth segregates at the surface of the nanoparticles, acting as a preferential adsorption/reaction site for the oxygenate. The addition of bismuth also shows a low amount of oxidized platinum, proving that bismuth protects platinum from oxidation, whereas on the monometallic Pt catalyst hydrogen pretreatment at 400 °C is essential to reduce the platinum and generate active sites for the reaction. In order to understand why the guaiacol conversion on the Pt catalyst drops from 80 to 20% within 6 h on stream whereas it is stable at around 60% on the PtBi catalyst, we compared the evolution of the Pt/C, Bi/C, and Pt/Bi ratios under different reaction conditions. Our results show that bismuth stabilizes the nanoparticles (negligible sintering observed) and prevents the formation of coke under oxidizing conditions. Conversely, coke formation

DOI: 10.1021/acscatal.8b04699
ACS Catal. 2019, 9, 3694−3699

and sintering take place on the monometallic Pt catalyst, blocking the catalytically active sites and leading to a rapid deactivation. These findings are in line with studies that ascribe the promotional effects of bismuth as decreasing oxidation of the active component platinum and at the same time restricting accumulation of carbon on the surface of the catalyst.

EXPERIMENTAL DETAILS

Using $H_2PtCl_6(H_2O)_6$ and $BiCl_3$, both >99.99% purity from Sigma-Aldrich, as precursors and 80−120 mesh activated carbon (AC) from Norit Americas Inc. as catalyst support, Pt and Bi were sequentially loaded by the wet impregnation method. Briefly, precursors were dissolved in HCl solution, followed by dropwise addition to the AC slurry and continued stirring for 8 h at room temperature (293 K). The catalysts were dried at 373 K in air before use in performance tests.

The APXPS measurements were performed in the solid−gas interface endstation[36] connected to the In Situ Spectroscopy beamline of the Swiss Light Source (SLS). The APXPS setup has a differentially pumped Scienta R4000 HiPP-2 analyzer. The photoelectrons were detected at an angle of 30° with respect to the direction of the surface normal. Linearly polarized light was used during all experiments. The available photon energy for NanoXAS is 250−1800 eV. The Pt 4f, Bi 4f, and C 1s spectra were all recorded using 650 eV excitation energy. After subtraction of a Shirley background, the photoemission peaks were deconvoluted using Voigt-shaped functions (for details see Table S5). An asymmetric Doniach−Sunjic line shape[37] was used to fit the metallic platinum component of the Pt 4f peaks. The position (binding energy scale), full width at half-maximum, and line shapes were constrained during the deconvolution of peak components associated with the same oxidation state (e.g., Pt^0 and Pt^{2+} in Figure S3). The catalyst powders were dispersed in ethanol and drop-casted as thin layers on 0.1 mm thin gold foils. The gold foil was clamped to the manipulator head by tantalum clips. The sample was heated by an IR laser, which projects at the back side of the sample holder. The temperature was monitored by a Pt100 sensor.

The experimental chamber has a flow tube configuration, which allows a fast exchange of gases in the cell. In the upstream, a gas line (3 mm diameter tube) with mass flow controllers for definite gases was connected. Guaiacol vapor was generated by heating the pure liquid (Acros organics, >99%) in a vial to 453 K in a vapor generator connected upstream to the flow tube. The lower side of the cell was connected to a 27 m^3/h root pump by a diaphragm valve. The pressure in the ambient-pressure cell was monitored by means of Baratron capacitance measurement units.

ASSOCIATED CONTENT

Supporting Information

The Supporting Information is available free of charge on the ACS Publications website at DOI: 10.1021/acscatal.8b04699.

Method details and results of characterization for the samples by means of the Brunauer−Emmett−Teller (BET) method, inductively coupled plasma-atomic emission spectroscopy (ICP-AES), transmission electron microscopy (TEM), temperature-programmed oxidation (TPO), transmission electron microscopy-energy dispersive X-ray analysis (TEM-EDX), and XPS, TEM images of the samples, performance of the catalysts with respect to guaiacol deoxygenation, XPS of Pt 4f of the samples in different reaction environments, the Pt 4f/C 1s, Bi 4f/C 1s, and Pt 4f/Bi 4f ratios evaluated under different reaction conditions, TEM-EDX results of PtBi, and temperature-programmed oxidation (TPO) profiles (PDF)

AUTHOR INFORMATION

Corresponding Author

*E-mail for L.A.: luca.artiglia@psi.ch.

ORCID

Kanak Roy: 0000-0003-0802-7710
Luca Artiglia: 0000-0003-4683-6447
Yang Xiao: 0000-0003-1705-2213
Arvind Varma: 0000-0002-3472-5929
Jeroen A. van Bokhoven: 0000-0002-4166-2284

Notes

The authors declare no competing financial interest.

ACKNOWLEDGMENTS

A.V. acknowledges support of the R. Games Slayter fund. We thank Yuan Wang for help with some experiments.

REFERENCES

(1) Elliott, D. C.; Baker, E. G.; Beckman, D.; Solantausta, Y.; Tolenhiemo, V.; Gevert, S. B.; Hörnell, C.; Östman, A.; Kjellström, B. Technoeconomic Assessment of Direct Biomass Liquefaction to Transportation Fuels. *Biomass* **1990**, *22*, 251−269.

(2) Furimsky, E. Catalytic Hydrodeoxygenation. *Appl. Catal., A* **2000**, *199*, 147−190.

(3) Bu, Q.; Lei, H.; Zacher, A. H.; Wang, L.; Ren, S.; Liang, J.; Wei, Y.; Liu, Y.; Tang, J.; Zhang, Q.; Ruan, R. A Review of Catalytic Hydrodeoxygenation of Lignin-Derived Phenols from Biomass Pyrolysis. *Bioresour. Technol.* **2012**, *124*, 470−477.

(4) He, Z.; Wang, X., Hydrodeoxygenation of Model Compounds and Catalytic Systems for Pyrolysis Bio-Oils Upgrading. In *Catalysis for Sustainable Energy*; de Gruyter: 2012; Vol. *1*, p 28.

(5) Mortensen, P. M.; Grunwaldt, J. D.; Jensen, P. A.; Knudsen, K. G.; Jensen, A. D. A Review of Catalytic Upgrading of Bio-Oil to Engine Fuels. *Appl. Catal., A* **2011**, *407*, 1−19.

(6) Saidi, M.; Samimi, F.; Karimipourfard, D.; Nimmanwudipong, T.; Gates, B. C.; Rahimpour, M. R. Upgrading of Lignin-Derived Bio-Oils by Catalytic Hydrodeoxygenation. *Energy Environ. Sci.* **2014**, *7*, 103−129.

(7) Wang, H.; Male, J.; Wang, Y. Recent Advances in Hydrotreating of Pyrolysis Bio-Oil and Its Oxygen-Containing Model Compounds. *ACS Catal.* **2013**, *3*, 1047−1070.

(8) Wang, Y.; De, S.; Yan, N. Rational Control of Nano-Scale Metal-Catalysts for Biomass Conversion. *Chem. Commun.* **2016**, *52*, 6210−6224.

(9) Zacher, A. H.; Olarte, M. V.; Santosa, D. M.; Elliott, D. C.; Jones, S. B. A Review and Perspective of Recent Bio-Oil Hydrotreating Research. *Green Chem.* **2014**, *16*, 491−515.

(10) Xiao, Y.; Varma, A. Catalytic Deoxygenation of Guaiacol Using Methane. *ACS Sustainable Chem. Eng.* **2015**, *3*, 2606−2610.

(11) Amen-Chen, C.; Pakdel, H.; Roy, C. Production of Monomeric Phenols by Thermochemical Conversion of Biomass: a Review. *Bioresour. Technol.* **2001**, *79*, 277−299.

(12) Xiao, Y.; Varma, A. Kinetics of Guaiacol Deoxygenation Using Methane over the Pt−Bi Catalyst. *React. Chem. Eng.* **2017**, *2*, 36−43.

(13) Xiao, Y.; Varma, A. Bio Oil Upgrading Using Methane: a Mechanistic Study of Reactions of Model Compound Guaiacol over Pt-Bi Bimetallic Catalyst. *ACS Sustainable Chem. Eng.* **2018**, *6*, 17368−17375.

DOI: 10.1021/acscatal.8b04699
ACS Catal. 2019, 9, 3694−3699

(14) Mallat, T.; Bodnar, Z.; Bronnimann, C.; Baiker, A. Platinum-Catalyzed Oxidation of Alcohols in Aqueous Solutions. The Role of Bi-Promotion in Suppression of Catalyst Deactivation. *Stud. Surf. Sci. Catal.* **1994**, *88*, 385−92.
(15) Mallat, T.; Baiker, A. Oxidation of Alcohols with Molecular Oxygen on Platinum Metal Catalysts in Aqueous Solutions. *Catal. Today* **1994**, *19*, 247−83.
(16) Hronec, M.; Cvengrosova, Z.; Tuleja, J.; Ilavsky, J. Liquid-Phase Oxidation of Hydrocarbons and Alcohols Catalyzed by Heterogeneous Palladium and Platinum Catalysts. *Stud. Surf. Sci. Catal.* **1990**, *55*, 169−176.
(17) Hendriks, H. E. J.; Kuster, B. F. M.; Marin, G. B. The Effect of Bismuth on the Selective Oxidation of Lactose on Supported Palladium Catalysts. *Carbohydr. Res.* **1990**, *204*, 121−129.
(18) Wenkin, M.; Ruiz, P.; Delmon, B.; Devillers, M. The Role of Bismuth as Promoter in Pd−Bi Catalysts for the Selective Oxidation of Glucose to Gluconate. *J. Mol. Catal. A: Chem.* **2002**, *180*, 141−159.
(19) Xiao, Y.; Greeley, J.; Varma, A.; Zhao, Z.-J.; Xiao, G. An Experimental and Theoretical Study of Glycerol Oxidation to 1,3-Dihydroxyacetone over Bimetallic Pt-Bi Catalysts. *AIChE J.* **2017**, *63*, 705−715.
(20) Starr, D.; Liu, Z.; Hävecker, M.; Knop-Gericke, A.; Bluhm, A. Investigation of Solid/Vapor Interfaces Using Ambient Pressure X-Ray Photoelectron Spectroscopy. *Chem. Soc. Rev.* **2013**, *42*, 5833−5857.
(21) Trotochaud, L.; Head, A. R.; Karslioglu, O.; Kyhl, L.; Bluhm, H. Ambient Pressure Photoelectron Spectroscopy: Practical Considerations and Experimental Frontiers. *J. Phys.: Condens. Matter* **2017**, *29*, 053002.
(22) Karslioglu, O.; Bluhm, H. In *Operando Research in Heterogeneous Catalysis*; Springer Verlag: 2017; pp 31−57.
(23) Salmeron, M. From Surfaces to Interfaces: Ambient Pressure XPS and Beyond. *Top. Catal.* **2018**, *61*, 2044−2051.
(24) Roy, K.; Artiglia, L.; van Bokhoven, J. A. Ambient Pressure Photoelectron Spectroscopy: Opportunities in Catalysis from Solids to Liquids and Introducing Time Resolution. *ChemCatChem* **2018**, *10*, 666−682.
(25) Artiglia, L.; Orlando, F.; Roy, K.; Kopelent, R.; Safonova, O.; Nachtegaal, M.; Huthwelker, T.; van Bokhoven, J. A. Introducing Time Resolution to Detect Ce^{3+} Catalytically Active Sites at the Pt/CeO_2 Interface through Ambient Pressure X-ray Photoelectron Spectroscopy. *J. Phys. Chem. Lett.* **2017**, *8*, 102−108.
(26) Raabe, J.; Tzvetkov, G.; Flechsig, U.; Böge, M.; Jaggi, A.; Sarafimov, B.; Vernooij, M. G. C.; Huthwelker, T.; Ade, H.; Kilcoyne, D.; Tyliszczak, T.; Fink, R. H.; Quitmann, C. PolLux: A New Facility for Soft X-Ray Spectromicroscopy at the Swiss Light Source. *Rev. Sci. Instrum.* **2008**, *79*, 113704.
(27) Du, W.; Su, D.; Wang, Q.; Frenkel, A. I.; Teng, X. Promotional Effects of Bismuth on the Formation of Platinum−Bismuth Nanowires Network and the Electrocatalytic Activity toward Ethanol Oxidation. *Cryst. Growth Des.* **2011**, *11*, 594−599.
(28) Besson, M.; Gallezot, P. In *Oxidation of Alcohols and Aldehydes on Metal Catalysts*; Wiley-VCH: 2001; pp 491−506.
(29) Okamoto, H. The Bi-Pt (Bismuth-Platinum) System. *J. Phase Equilib.* **1991**, *12*, 207−210.
(30) Ermakova, M. A.; Ermakov, D. Y.; Kuvshinov, G. G.; Plyasova, L. M. New Nickel Catalysts for the Formation of Filamentous Carbon in the Reaction of Methane Decomposition. *J. Catal.* **1999**, *187*, 77−84.
(31) Zhang, Y.; Smith, K. J. Carbon Formation Thresholds and Catalyst Deactivation During CH_4 Decomposition on Supported Co and Ni Catalysts. *Catal. Lett.* **2004**, *95*, 7−12.
(32) Wang, S.; Lu, G. Q. Catalytic Activities and Coking Characteristics of Oxides-Supported Ni Catalysts for CH_4 Reforming with Carbon Dioxide. *Energy Fuels* **1998**, *12*, 248−256.
(33) Burke, G. M.; Wurster, D. E.; Berg, M. J.; Veng-Pedersen, P.; Schottelius, D. D. Surface Characterization of Activated Charcoal by X-Ray Photoelectron Spectroscopy (XPS): Correlation with Phenobarbital Adsorption Data. *Pharm. Res.* **1992**, *09*, 126−130.
(34) Zhu, T.; Flytzani-Stephanopoulos, M. Catalytic Partial Oxidation of Methane to Synthesis Gas over Ni−CeO_2. *Appl. Catal., A* **2001**, *208*, 403−417.
(35) Son, I. H.; Lee, S. J.; Song, I. Y.; Jeon, W. S.; Jung, I.; Yun, D. J.; Jeong, D.-W.; Shim, J.-O.; Jang, W.-J.; Roh, H.-S. Study on Coke Formation Over Ni/γ-Al_2O_3, Co-Ni/γ-Al_2O_3, and Mg-Co-Ni/γ-Al_2O_3 Catalysts for Carbon Dioxide Reforming of Methane. *Fuel* **2014**, *136*, 194−200.
(36) Orlando, F.; Waldner, A.; Bartels-Rausch, T.; Birrer, M.; Kato, S.; Lee, M.-T.; Proff, C.; Huthwelker, T.; Kleibert, A.; van Bokhoven, J.; Ammann, M. The Environmental Photochemistry of Oxide Surfaces and the Nature of Frozen Salt Solutions: A New in Situ XPS Approach. *Top. Catal.* **2016**, *59*, 591−604.
(37) Doniach, S.; Sunjic, M. Many-Electron Singularity in X-Ray Photoemission and X-Ray Line Spectra from Metals. *J. Phys. C: Solid State Phys.* **1970**, *3*, 285−291.

DOI: 10.1021/acscatal.8b04699
ACS Catal. 2019, 9, 3694−3699

Supporting Information

Role of Bismuth in the Stability of Pt-Bi Bimetallic Catalyst for Methane Mediated Deoxygenation of Guaiacol, an APXPS Study

*Kanak Roy[a], Luca Artiglia[*b,c], Yang Xiao[d], Arvind Varma[d], Jeroen A. van Bokhoven[a,b]*

[a]Institute for Chemical and Bioengineering, ETH Zürich, 8093 Zurich (Switzerland).

[b]Laboratory for Catalysis and Sustainable Chemistry, Paul Scherrer Institute, Forschungsstrasse 111, 5232 Villigen (Switzerland).

[c]Laboratory of Environmental Chemistry, Paul Scherrer Institute, Forschungsstrasse 111, 5232 Villigen (Switzerland).

[d]Davidson School of Chemical Engineering, Purdue University, West Lafayette, IN 47907 (USA).

[*]Email: luca.artiglia@psi.ch;

EXPERIMENTAL DETAILS

Using $H_2PtCl_6(H_2O)_6$ and $BiCl_3$, both > 99.99% purity from Sigma Aldrich, as precursors and 80–120 mesh activated carbon (AC) from Norit Americas Inc. as catalyst support, Pt and Bi were sequentially loaded by the wet impregnation method. Briefly, precursors were dissolved in HCl solution, followed by dropwise addition to the AC slurry and continued stirring for 8 h at room temperature (293 K). The catalysts were dried at 373 K in air before use in performance tests.

The ambient pressure x-ray photoelectron spectroscopy (APXPS) measurements were performed in the solid-gas interface endstation[1] connected to the In Situ Spectroscopy beamline of the Swiss Light Source (SLS). The APXPS setup has a differentially pumped Scienta R4000 HiPP-2 analyzer. The photoelectrons were detected at an angle of 30° with respect to the direction of the surface normal. Linearly polarized light was used during all experiments. The available photon energy for NanoXAS is 250-1800 eV. The Pt 4f, Bi 4f, and C 1s spectra were all recorded using 650 eV excitation energy. After subtraction of a Shirley background, the photoemission peaks were deconvoluted using Voigt shaped functions. Asymmetric Doniach-Sunjic line shape[2] was used to fit the metallic platinum component of the Pt 4f peaks. The position (binding energy scale), full width at half maximum and the line-shapes were constrained during the deconvolution of peak components associated with the same oxidation state (e.g. Pt^0 and Pt^{2+} in Figure S3). The powder catalysts were dispersed in ethanol and drop-casted as a thin layer on a 0.1 mm thin gold foil. The gold foil was clamped to the manipulator head by tantalum clips. The sample was heated by an IR laser, which projects at the back side of the sample holder. The temperature was monitored by a Pt100 sensor. The experimental chamber has a flow tube configuration, which allows a fast exchange of gases in the cell. In the upstream, a gas line (3

mm diameter tube) with mass flow controllers for definite gases was connected. Guaiacol vapor was generated heating the pure liquid (Acros organics, >99%) in a vial to 453 K in a vapor generator connected upstream to the flow tube. The lower side of the cell was connected to a 27 m3/h root pump by a diaphragm valve. The pressure in the ambient pressure cell was monitored by means of Baratron capacitance measurement units.

By N_2 adsorption and desorption at 77 K via a Micromeritics ASAP 2020 apparatus, Brunauer-Emmett-Teller (BET) measurements were conducted, giving physisorption properties of catalysts, including surface area, pore size and pore volume. Prior to measurements, degassing was carried out at 300 °C for 8 h. Using 0.5 wt% Pt/Al_2O_3 as calibration standard, Pt dispersion was obtained by the H_2-O_2 titration approach. Note that at room temperature, Bi does not adsorb H_2 molecules and bismuth oxide does not react with H_2. The transmission electron microscopy (TEM) scans were operated at 200 kV with LaB_6 source (FEI-Tecnai). The TEM samples were prepared by suspending fine catalyst particles in ethanol, followed by dispersing them on 200 copper mesh grids with lacey carbon film coating, and then drying in air at room temperature. The TEM-EDX scans were carried out using a FEI Talos F200X scanning transmission electron microscope. Energy dispersive x-ray analysis (EDX) was done using X-FEG high-brightness electron source. Elemental analysis of catalysts was carried out by the inductively coupled plasma-atomic emission spectroscopy (ICP-AES) method using a SPECTRO Instrument. In the temperature programmed oxidation (TPO) process, 5% O_2 in N_2 gas mixture was used as the oxidizing gas. The used catalysts were packed in the reactor for TPO measurements without any pretreatment. The heating rate was 5 °C/min and the standard catalyst packed weight was 0.25-0.50 g. The total gas flow rate was 100 mL/min. The O_2 consumption was measured by a binary gas analyzer equipped with a thermal conductivity detector (TCD).

Table S1. BET Characterization Results of Various Catalytic Materials

Catalyst	BET Surface Area, m^2/g	Pore Size, nm	Pore Volume, cm^3/g
5% Pt	501	3.5	1.5
5% Pt-2% Bi	497	3.1	1.0
2% Bi	511	2.6	0.7
used 5% Pt	377	1.9	0.8
used 5% Pt-2% Bi	461	2.7	0.9

Table S2. ICP-AES Element Analysis of Various Catalytic Materials

Catalyst	Pt % (fresh)	Bi % (fresh)	Pt % (used)	Bi % (used)
5% Pt	4.92	-	4.85	-
5% Pt-2% Bi	5.18	1.92	5.08	1.88
2% Bi	-	2.03	-	1.98

Table S3. TEM and H_2-O_2 Titration Results for Various Catalytic Materials

	Particle Size, nm		
Catalyst	TEM	H_2-O_2 Titration	Pt Dispersion, %
5% Pt	4.4	4.2	19.7
5% Pt-2% Bi	3.3	3.1	24.5
2% Bi	3.9	-	-
Used 5% Pt	5.6	4.9	14.3
Used 5% Pt-2% Bi	3.5	3.2	21.9

Table S4. Peak Positions and Coke Amounts from Temperature-Programmed Oxidation (TPO) Experiments

	Peak Position, °C			
Catalyst (wt%)	I	II	III	Accumulated Coke, mg/g_{cat}
Used 5% Pt	450	550	580	523.2
Used 5% Pt-2% Bi	450	-	580	36.6

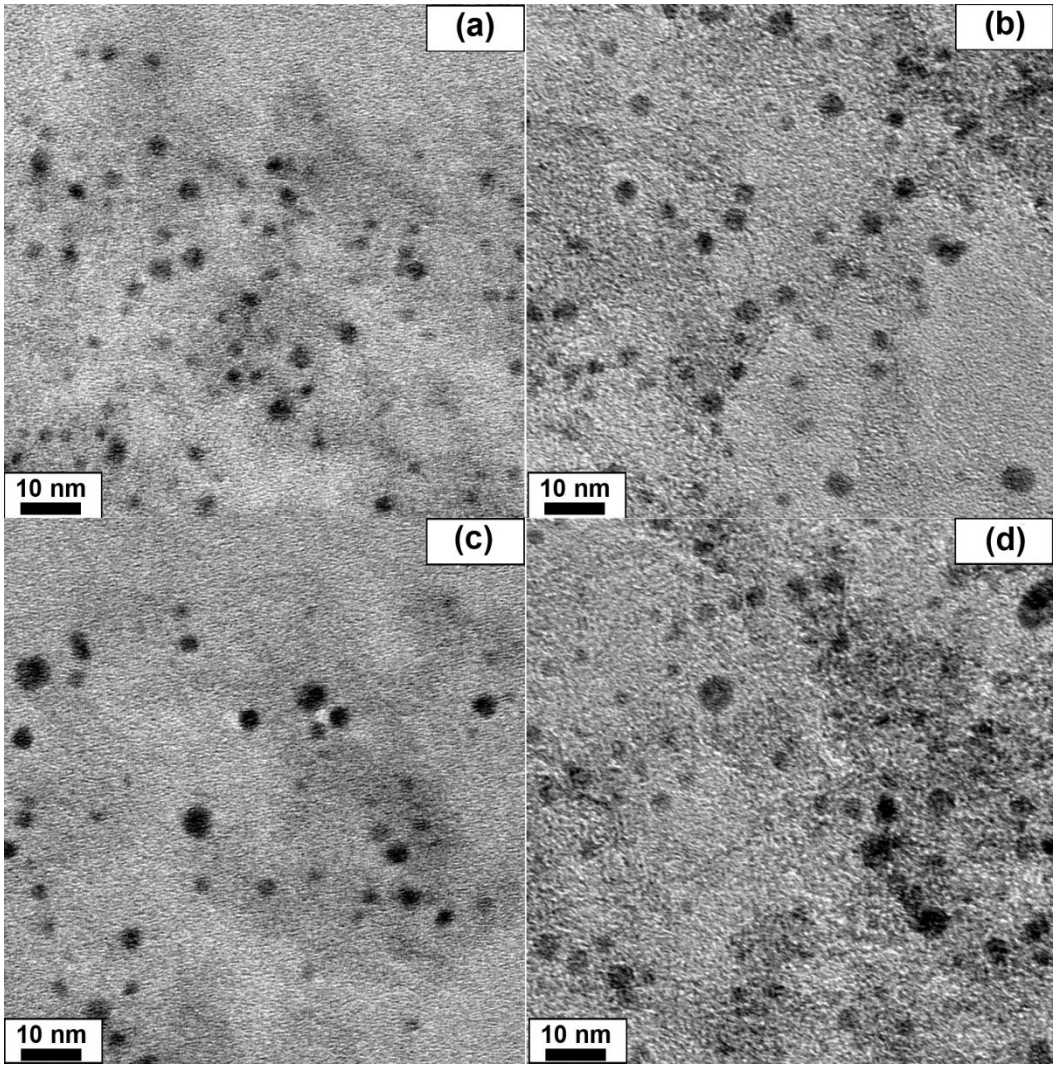

Figure S1. TEM images of a) fresh 5% Pt, b) fresh 5% Pt-2% Bi, c) used 5% Pt and d) used 5% Pt-2% Bi catalysts.

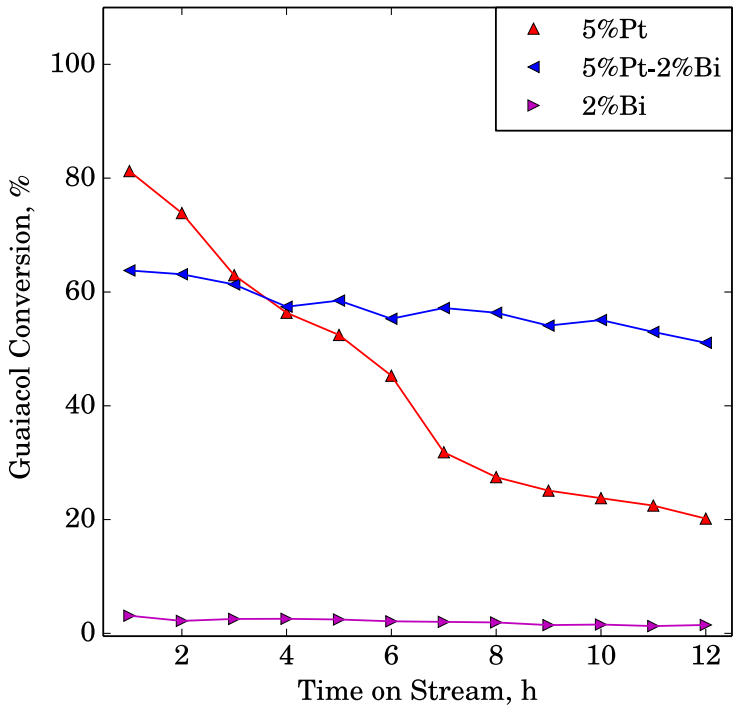

Figure S2. Guaiacol deoxygenation performance using methane over various catalysts, 673K, 0.5 g catalyst, 50 ml/min methane, 50 ml/min nitrogen, 0.025 ml/min guaiacol (liquid, room temperature). In gaseous phase, the ratio of methane to guaiacol is about 10, similar to the value used for APXPS.

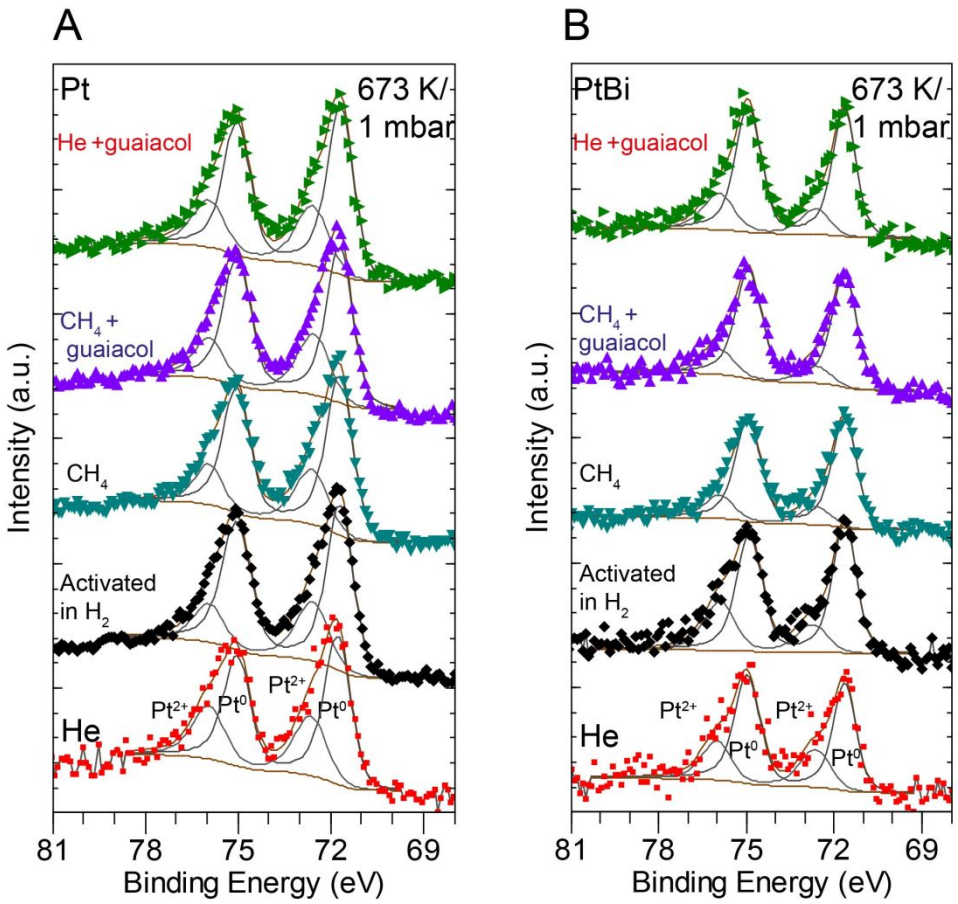

Conditions	Pt^{2+}/Pt^{0}
Unactivated catalyst	0.48
Activated catalyst	0.43
in CH_4	0.41
in CH_4 + guaiacol	0.47
in He + guaiacol	0.43

Conditions	Pt^{2+}/Pt^{0}
Unactivated catalyst	0.45
Activated catalyst	0.26
in CH_4	0.19
in CH_4 + guaiacol	0.18
in He + guaiacol	0.23

Figure S3. The evolution of Pt 4f in A) Pt/AC and in B) Pt-Bi/AC catalysts recorded at 673K and at a total pressure of 1 mbar at various conditions.

Table S5. Details of the peaks used for the deconvolution of the photoemission spectra of Bi 4f, Pt 4f and C 1s.

Spectral Region	Components	Binding Energy (eV)	FWHM (eV)
Pt $4f_{7/2}$	Pt^0	71.6-71.7	0.9-1
	Pt^{2+}	72.6	1.1-1.2
Bi $4f_{7/2}$	Bi^0	157.6	0.9-1
	Bi^{3+}	159.7	1.1-1.3
C 1s	sp^3 carbon	284.9-285	1.1
	-C-O, -C-O-C	286.3	1.1-1.2
	Gas phase methane	286.6	0.8
	-C=O	287.5	1.1-1.2

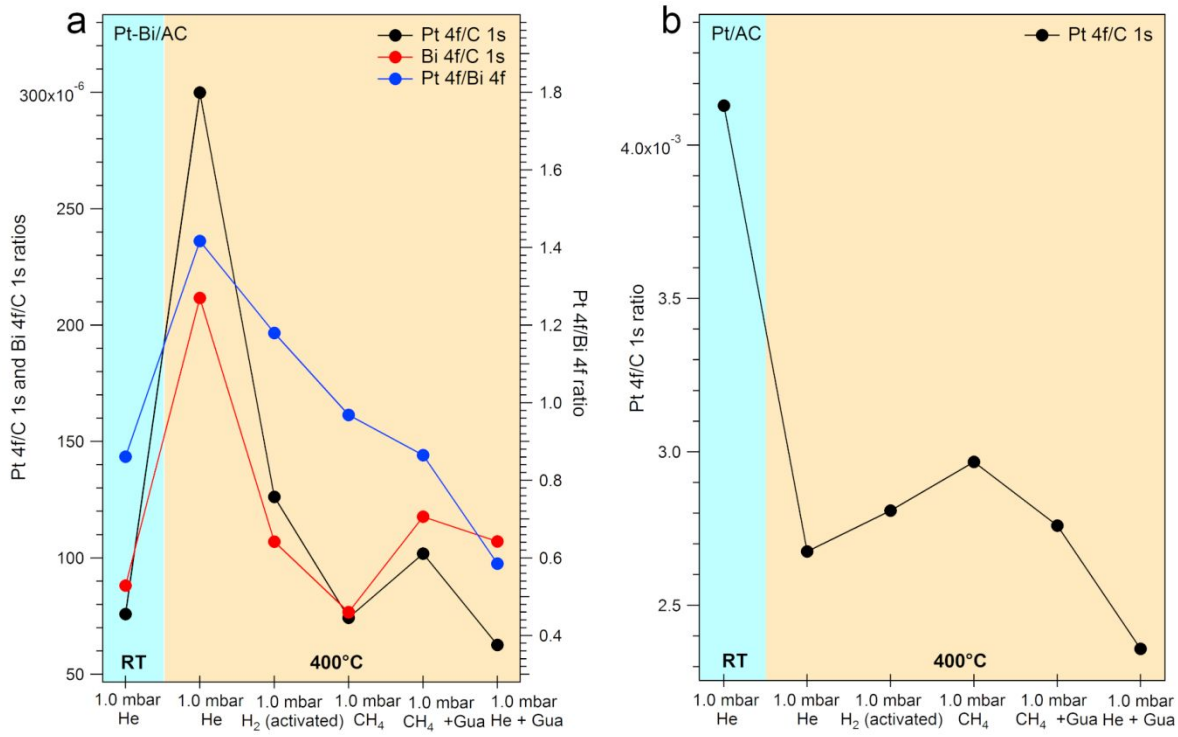

Figure S4. (a) Left y-axis: evolution of the ratios between the area of the Pt 4f and Bi 4f photoemission signal and that of the 285.0 eV component of the C 1s with the reaction conditions on the PtBi sample. Right y-axis: evolution of the ratio between the area of the Pt4f and that of the Bi 4f with the reaction conditions on the PtBi sample. (b) Evolution of the ratio between the area of the Pt 4f and that of the 285.0 eV component of the C 1s with the reaction conditions on the Pt sample The areas were normalized to the relative sensitivity factors (RSF) of each element.

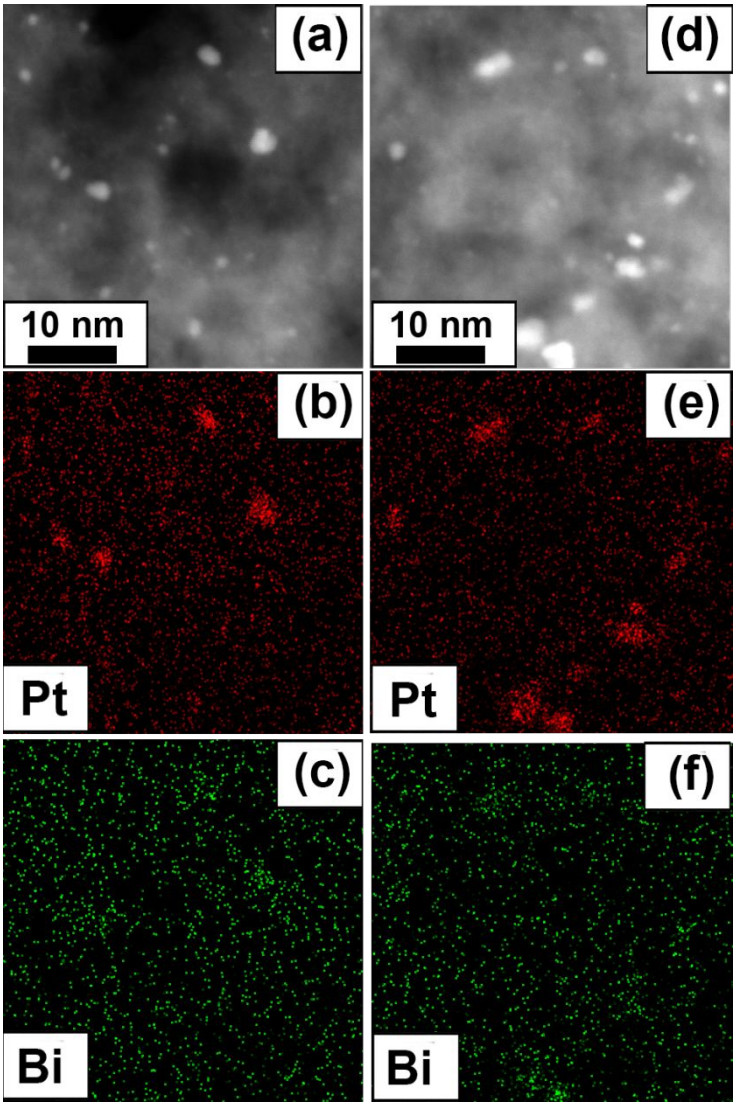

Figure S5. (a-c) TEM scan and Pt, Bi EDX mapping for fresh PtBi, (d–f) TEM scan and Pt, Bi EDX mapping for used PtBi catalysts

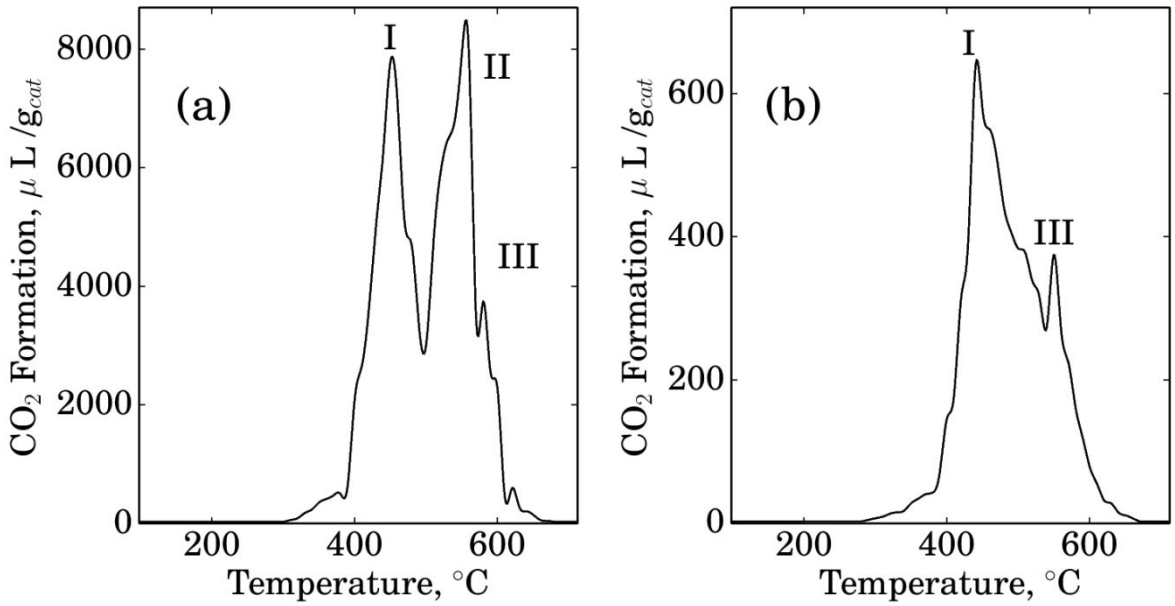

Figure S6. Temperature-Programmed Oxidation (TPO) Profiles for (a) Used 5% Pt and (b) Used 5% Pt-2% Bi Catalysts.

REFERENCES

(1) Orlando, F.; Waldner, A.; Bartels-Rausch, T.; Birrer, M.; Kato, S.; Lee, M.-T.; Proff, C.; Huthwelker, T.; Kleibert, A.; van Bokhoven, J.; Ammann, M. The Environmental Photochemistry of Oxide Surfaces and the Nature of Frozen Salt Solutions: A New in Situ XPS Approach. *Top. Catal.* **2016**, *59*, 591-604.

(2) Doniach, S.; Sunjic, M. Many-Electron Singularity in X-Ray Photoemission and X-Ray Line Spectra from Metals. *J. Phys. C* **1970**, *3*, 285-291.